RSC Sustainability

ROYAL SOCIETY OF CHEMISTRY

PAPER

View Article Online
View Journal | View Issue

Cite this: *RSC Sustainability*, 2025, **3**, 4703

Functionalized AuNP-mycelial composites as engineered living materials for sustainable mercury remediation

Juwon S. Afolayan and Carole C. Perry *

Heavy metal contamination, particularly mercury (Hg^{2+}), poses severe environmental and health risks even at trace levels. Current methods face challenges such as high costs, secondary pollution, and structural complexity, which limit global adaptability. This study presents a naturally templated engineered living material (ELM) using *Aspergillus niger* mycelia functionalized with gold nanoparticles (AuNPs) for effective mercury bioremediation. A rapid colorimetric detection system using surface-modified AuNPs, either with conventional reductant (borate), nutrient (glucose), antibiotic (cefaclor), or ionic compound (citrate), achieved a response within 5 seconds with a detection limit down to 5 μM. Biofilters generated from AuNP-bound mycelia demonstrated efficient mercury removal, reducing Hg^{2+} from 5 ppb to 0.5 ppb, outperforming conventional polyethylene filters (Pierce™ 30 μM), and meeting World Health Organization (WHO) safety standards. The material maintained consistent performance over five reuse cycles (without any structural deformation, allowing for additional use cycles), with progressive mercury desorption for potential recovery. Growth conditions (nitrogen sources, AuNP concentration, surface functionalization, and duration of growth) could be used to influence AuNP assembly, fungal physiology, and activity of the composite materials. This scalable and cost-effective approach integrates nanotechnology with fungal bioremediation, providing a sustainable, adaptable solution for heavy metal pollution control.

Received 25th June 2025
Accepted 17th August 2025

DOI: 10.1039/d5su00556f

rsc.li/rscsus

Sustainability spotlight

This contribution addresses key sustainability principles in science and engineering, including waste minimization, eco-friendly material design, and the development of degradable functional materials for environmental remediation. Specifically, we demonstrate nanomaterial-enabled remediation of mercury involving both detection and removal, aligning with SDG 3 (Good Health and Well-being) and SDG 6 (Clean Water and Sanitation), incorporate green synthesis and functionalization approaches using biologically derived materials and surface modifiers (glucose, citrate, cefaclor, and borate) for the generation of functional nanomaterials, supporting SDG 9 (Industry, Innovation and Infrastructure), emphasize reusability, recyclability, and system scalability, contributing to circular economy strategies in line with SDG 12 (Responsible Consumption and Production), and finally, we provide insights into how biopolymer surface chemistry influences nanoparticle assembly and bioremediation, supporting SDG 9.

1 Introduction

Environmental monitoring is crucial for detecting and removing contaminants to ensure human and ecosystem safety.[1] Common toxicants include heavy metals, pesticides, oil residues, and antimicrobial-resistant organisms.[2,3] These contaminants often enter water bodies, posing significant health risks even at low concentrations.[4,5]

Mercury (Hg^{2+}) is particularly hazardous, with toxicity risks even at concentrations slightly above regulatory limits of 1–2 pbb.[5] Current remediation methods, such as chemical precipitation, adsorption, ion-exchange columns, and activated carbon filtration, are often costly, have limited selectivity, require strong chemicals, and can cause secondary pollution.[6,7] An ideal next-generation filtration system must be sustainable, cost-effective, scalable, reusable, and environmentally friendly, while ensuring high removal efficiency suitable for application across diverse economic settings.[8]

Nanomaterials are widely used in environmental monitoring due to their unique optical and adsorptive properties.[9,10] Metal-based nanoparticles (NPs), especially gold nanoparticles (AuNPs), have shown strong potential for mercury adsorption.[11] However, most nanoparticle-based approaches rely on chemically intensive functionalization methods or matrices (supportive mediums that embed the NPs), which often involve hazardous chemicals and energy-intensive processes, thereby limiting their environmental compatibility.[12]

Interdisciplinary Biomedical Research Centre, Department of Chemistry and Forensics, School of Science and Technology, Nottingham Trent University, Nottingham NG11 8NS, UK. E-mail: carole.perry@ntu.ac.uk

Inspired by the natural gold accumulation ability of *Fusarium oxysporum*,[13] we tested if *A. niger*, a robust, globally adaptable, and well-studied fungus with similar ecology to *F. oxysporum*[14], could replicate or enhance bio-nanocomposite formation while eliminating the need for synthetic modification techniques. Unlike previous studies that focus solely on mercury detection, we integrated removal, reusability, and recyclability using engineered living materials by templating *A. niger* mycelia as a functional matrix for gold nanoparticle immobilization. This innovation bridges biosorption and nanotechnology, enabling both colorimetric mercury detection (using surface-functionalized AuNPs alone) and efficient mercury remediation (using AuNP-functionalized mycelia) within a single system.

We have developed a versatile bio-nanocomposite optimized for real-world applications by tuning its microstructural properties through controlled growth conditions. This approach offers a sustainable, bio-based platform for gold nanoparticle functionalization without the use of harsh or environmentally unfriendly chemicals. It enables high-efficiency mercury filtration facilitated by gold nanoparticles with diverse surface properties. Furthermore, the material acts as a nature-inspired biofilter for Hg^{2+} removal, capable of multiple reuse cycles while maintaining a stable structure suitable for mercury recycling. This significantly advances conventional mercury monitoring systems.

Our goal was to develop fungal-templated gold nanoparticle–mycelial composites for sustainable mercury bioremediation. We investigated the effects of nitrogen sources (nitrate *vs.* glutamine) on the growth of the fungus, AuNP concentrations, and fungal growth duration on nanoparticle immobilization and Hg^{2+} removal efficiency to establish a scalable and adaptable strategy. To explore how surface chemistry influences performance, we used four distinct capping agents: borate (a conventional reductant), glucose (a nutrient and green stabilizer), citrate (an ionic stabilizer), and cefaclor (a repurposed antibiotic with potential bioactivity). This approach integrates detection, removal, and reusability into a single platform, advancing comprehensive monitoring technologies with global applicability.

2 Materials

A. niger (A1144) was provided by Dr Matthias Brock, Nottingham University. Gold nanoparticles (AuNPs) capped with either borate, glucose, cefaclor, or citrate were synthesized in-house, with their properties detailed in a previous publication (Sadaf *et al.*, 2024).[15] Potato dextrose agar (PDA) (70 139), sodium nitrate (7631-99-4), glutamine (56-85-9), phosphate buffer saline (PBS) (P4417), mercury standard for ICP (28 941), HNO_3 (7697-37-2), and HCl (7647-01-0) were purchased from Sigma-Aldrich UK. All reagents were prepared according to the manufacturer's instructions.

3 Methods

3.1 Fungal culture conditions

A. niger was sub-cultured on potato dextrose agar (PDA) at 25 °C. The freshly grown fungus was stored as a mother culture at 4 °C. For experiments, spores were harvested after 3–5 days of growth on PDA, washed with phosphate-buffered saline (PBS), and counted using a hemocytometer (NanoEntek C-Chip disposable) to prepare the desired spore concentration.[15] *Aspergillus* strains utilize various nitrogen sources,[16] with glutamine playing a key role in early growth within the first 24 hours, supporting *A. niger*'s initial development without additional activators.[17] Nitrate, also well-utilized by *A. niger*,[16] serves as a useful comparison.

The methods for gold nanoparticle (AuNP) deposition on fungal mycelium, preparation of the AuNP-Mycelia composite sample for analyses, evaluation of AuNP incorporation into fungal mycelia by Scanning Electron Microscopy/Energy Dispersive X-ray Spectroscopy (SEM/EDX), and determination of gold concentration on mycelium using Inductively Coupled Plasma Mass Spectrometry (ICPMS) were as reported in our previous study;[15] information is also provided in the SI (SI). The AuNPs with different surface modifications (ionic-citrate, nutrient-glucose, antibiotic-cefaclor, and conventional reductant-sodium borohydride) were crystalline, spherical nanoparticles, with some triangular glucose-stabilized particles, all under 100 nm, and with high negative zeta potentials between −30 to −40 mV.[15] In this study, we have tested nitrate and glutamine as nitrogen sources for fungal growth and compared their effects. All other experimental conditions for the functionalization of *A. niger* with AuNPs remain as previously reported.

3.2 Quantification of inorganics on AuNPs and surface analysis

The temperature response of both ordinary fungal materials and their respective AuNPs was assessed using thermogravimetric analysis (TGA) using a TGA/DSC 3+ instrument from Mettler-Toledo International Inc., with samples heated in air at a rate of 10°C min^{-1} over the temperature range 30 °C to 900 °C.

3.3 Colorimetric sensing of mercury (Hg^{2+})

The colorimetric sensing of Mercury (Hg^{2+}) was accomplished using a spectrophotometric method (Cary 50 Bio Ultraviolet-Visible Spectrophotometer, Agilent Technologies). A range of different concentrations of the heavy metal (1, 2, 10, 20, 30, 40, 50 μM) was prepared and used in the experiments. The AuNPs system was combined with different concentrations of Hg^{2+} in equal volumes (1 : 1) and thoroughly mixed.[18] The absorbance of the resulting solution (2 mL) was transferred into a polystyrene Cuvette (SARSTEDT, 10 × 10 × 45 mm) and measured at 25 °C between 300 and 800 nm.

3.4 Physiological studies of *A. niger* under the effect of Au coated nanoparticles

Sporulation was studied in triplicate using a hemacytometer to count spores. Freshly grown mycelium was collected to gather spores and counted to determine the average number produced under different AuNP treatment conditions.

3.5 Biofiltration of mercury using AuNP-mycelia composite microstructure

A Pierce™ Centrifuge Column with a 30 μM polyethylene filter was used. 1 mL of 5 ppb Hg^{2+} was added to 0.01 g of AuNP-Mycelia composite, infiltrated for 30 min, and then centrifuged at 5000 rpm for 3 min. The filtrate was collected and digested in aqua regia, and Hg^{2+} was measured by ICPMS (NexION 100 ICP Mass Spectrophotometer).

3.6 Testing reusability of the AuNP-mycelia biofilters

Reusability was evaluated using ICP-MS. 1000 μL of 5 ppb mercury solution was run across 0.01 g of composite five times, centrifuged after 30 min, and diluted for ICP-MS analysis. DDH_2O at pH 8.0 was used to wash off attached mercury ions, collected, and the eluant analysed *via* ICP-MS.

3.7 Analysis and statistics

Experiments were performed in triplicate. Mean values and standard deviations from the experiment are reported. One-way or two-way ANOVA determined significant differences among treatment factors. Tukey's post hoc test was used for multiple comparisons ($P < 0.05$). Analyses were performed using GraphPad Prism 10.0 in triplicate, both technically and biologically.

4 Results and discussion

In this research study, a reusable biofilter for sustainable mercury bioremediation was developed using engineered living materials (ELM) from *Aspergillus niger* mycelia, which were bound to surface-functionalized gold nanoparticles (AuNPs) with different capping agents (borate, glucose, cefaclor, citrate). The study examined how growth conditions (nitrogen sources, growth duration, and AuNP concentration) influenced the morphological and chemical characteristics of the biofilter in relation to the effectiveness of the proposed biofilter. Characterization of the AuNPs and their efficiency in rapid mercury detection is described first, followed by analysis of the composite materials and their performance in mercury removal.

4.1 Surface characterization of gold nanoparticles by thermogravimetric analysis (TGA) for colorimetric detection of mercury

Thermogravimetric analysis (TGA) was used to assess the amount and extent of association between the capping agents and AuNPs. Thermograms revealing weight changes (TGA), temperature differences (DTA), and heat flow (DSC) during capping agent digestion[19] are presented in Fig. SF1. Table 1 lists the capping agent amounts on AuNPs as a % of the sample mass.

Table 1 Amount of capping material associated with different types of AuNPs

Type of AuNPs	Capping material	Amount (%)
$NaBH_4$-reduced AuNPs	Borate	51%
Glucose-reduced AuNPs	Glucose	91.4%
Cefaclor-reduced AuNPs	Cefaclor	25%
Citrate-stabilized AuNPs	Sodium citrate	46%

The major changes indicating capping agent interactions with the Au.

Au NPs include lower desorption and higher oxidation temperatures in $NaBH_4$-AuNPs (350–500 °C) compared to $NaBH_4$ alone (Fig. SF1A);[19] shifts in weight loss stages post-carbonation in Glc-AuNPs (400–550 °C), suggesting stronger interactions than free glucose (Fig. SF1B);[20] broader thermal degradation ranges in cefaclor-AuNPs, compared to cefaclor alone (Fig. SF1C); and altered decomposition patterns in Cit-AuNPs relative to citrate alone, suggesting binding (Fig. SF1D). Further description on the component losses during progressive pyrolysis is contained in Fig. SF1.

TGA results (Fig. SF1) showed that glucose (91.4%), $NaBH_4$ (51%), and citrate (46%) were present in significantly higher amounts on AuNPs as compared to cefaclor. Their high abundance, attributed to their reducing properties and/or hydroxyl groups, may enhance sensitivity for mercury detection, particularly through interactions such as the complexation or amalgamation of citrate with mercury ions.[21,22] $NaBH_4$-AuNPs, Cef-AuNPs, and Cit-AuNPs exhibited greater thermostability (Fig. SF1A, C, and D, respectively).

4.2 Mercury detection by surface functionalised AuNPs

Having evaluated surface compositions, the sensitivity of surface-functionalized gold nanoparticles (AuNPs) to mercury (Hg^{2+}) was assessed using UV-spectrophotometry within the concentration range of 1–50 μM (Fig. 1A–D). Rapid detection of Hg^{2+} (within 5 seconds) was observed, with changes in surface plasmon resonance (SPR) properties indicating distinct responses for each AuNP type. Images illustrating the colorimetric changes are shown in Fig. SF2.

Glucose-stabilized (Glc-AuNPs) and sodium borohydride-reduced ($NaBH_4$-AuNPs) AuNPs were able to detect Hg^{2+} at concentrations as low as 5 μM. Glc-AuNPs showed a band shift from 535 nm to 691 nm, while $NaBH_4$-AuNPs exhibited a broad shift from 524 nm to 605 nm. Cef-AuNPs (AuNPs with the antibiotic surface) had a detection limit of 20 μM, with no significant band shift at 528 nm. Cit-AuNP (with an ionic citrate surface) was sensitive down to 10 μM, with an absorption band decrease at 544 nm without significant shifts. Colour changes from brick red to purple ($NaBH_4$-AuNPs, Glc-AuNPs, Cit-AuNPs) and slightly pink (Cef-AuNPs) indicated nanoparticle aggregation due to metal ion binding,[23] Fig. SF2. The shift in SPR peaks indicates changes in the local dielectric environment and surface electron density. The binding of Hg^{2+} to surface-functionalized groups likely causes aggregation or changes in nanoparticle morphology, leading to observable shifts in absorption.[24]

The results are consistent with insights from TGA analyses, but $NaBH_4$-AuNPs outperformed Cit-AuNPs in Hg^{2+} detection (lower limit 5 μM), despite the relative abundance of citrate.

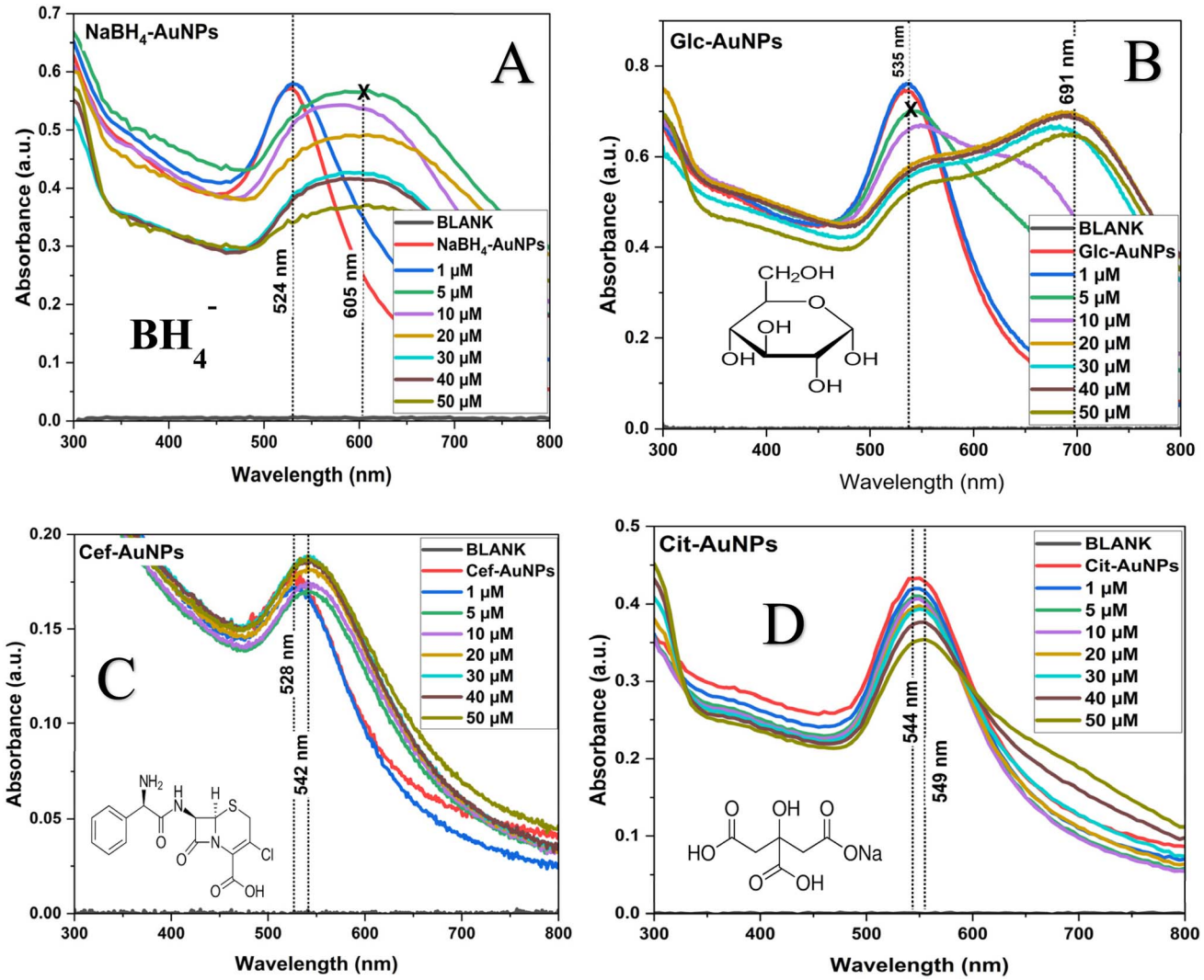

Fig. 1 UV-vis Spectroscopy of AuNPs interacting with mercury at different concentrations showing the absorption patterns of (A) $NaBH_4$-reduced AuNPs, (B) Glc-AuNPs, (C) Cef-AuNPs, and (D) Cit-AuNPs.

Literature indicates that colorimetric sensing of mercury by nanoparticles can achieve detection limits as low as 11.3 μM without complex modifications (*e.g.*, aptamers)[25], and as low as 0.7 nM with modifications such as 2-[4-(2-hydroxyethel) piperazine-1-yl] ethanesulfonic acid (HEPES).[26] This study highlights the excellent chemical specificity of AuNPs for Hg^{2+} detection, the unique detection patterns of individual surfaces, and the potential for customizing surface functionalization for rapid, visible, and sensitive mercury monitoring. Future studies could focus on improving detection times and colour changes for field applications.[27]

4.3 Studying the growth and properties of *A. niger* mycelium upon Au NP interaction under different nitrogen sources

4.3.1 Impact on the surface chemistry of mycelium. Surface chemistry characteristics such as wettability and surface free energy (SFE) can indicate how materials interact with bioactive agents (*e.g.*, AuNPs) or contaminants in solution (*e.g.*, mercury).[28] We investigated how different nitrogen sources (glutamine *vs.* nitrate) influence the surface properties of *A. niger* mycelia, which may provide insights into gold nanoparticle (AuNP) deposition, mercury filtration performance, and the recyclability of mercury from the resulting AuNP–mycelial composites. As shown in Fig. SF3, the media-facing side (MF) of mycelia grown with glutamine exhibited better wettability in water (Fig. SF3A). Diiodomethane also more readily wetted the face of active growth (GF) of glutamine-grown mycelia, suggesting a higher presence of non-polar surface groups compared to nitrate-grown mycelia (Fig. SF3B). Higher surface-free energy and surface energy distribution (polar and non-polar) in glutamine-grown mycelia may improve surface interactions, allowing for AuNP assembly and mercury removal (Fig. SF3C).

4.3.2 Impact on mycelium morphology and sporulation. AuNPs were introduced into *Aspergillus niger* cultures, where they were naturally incorporated into the fungal mycelium, forming templated engineered living materials (ELMs). This approach repurposed the AuNPs from their original role in

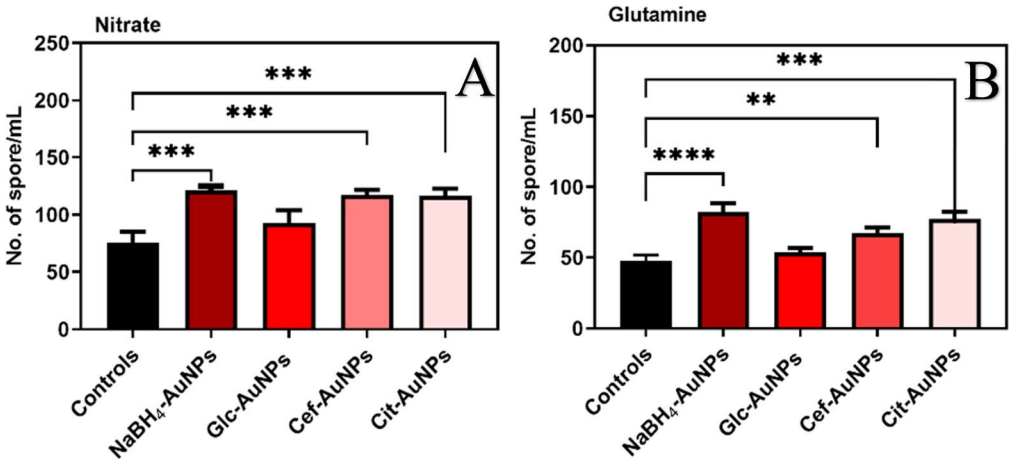

Fig. 2 Quantitative comparison of the physiological response of *Aspergillus niger* by sporulation at 30 μg mL^{-1} of AuNPs in (A) nitrate and (B) glutamine as nitrogen source. The level of significance: *($p \leq 0.05$), **($p \leq 0.01$), and ***($P \leq 0.001$).

mercury detection to a new function within the mycelia-AuNP composite for mercury removal. The mycelia showed physical and physiological changes, especially concerning sporulation, indicating fungal adjustment for AuNP deposition. After 10 days, the initial brick red colour of the AuNPs was only barely visible in the culture medium due to significant mycelial growth. This could be due to the fungal uptake of the AuNPs from the growth media.[15] Fungal growth was proportional to the initial AuNP concentration (20 or 30 μg mL^{-1}). Growth outcomes varied under the different growth conditions (Fig. SF4A–E).

To understand the physiological impact of the highest concentration of AuNPs (30 μg mL^{-1}) on *A. niger* due to AuNP introduction in the fungal culture, we evaluated sporulation under the different AuNP types in media with two different nitrogen sources, nitrate or glutamine (Fig. 2A and B). Both are known to support growth[29] and we recorded significant differences in behaviour (Fig. 2). Sporulation, a stress response and survival mechanism, significantly increased with AuNP exposure, except for growth in the presence of Glc-AuNPs. This could be because the glucose on the AuNP surface, being abundant (as indicated by TGA), provided an additional carbon source,

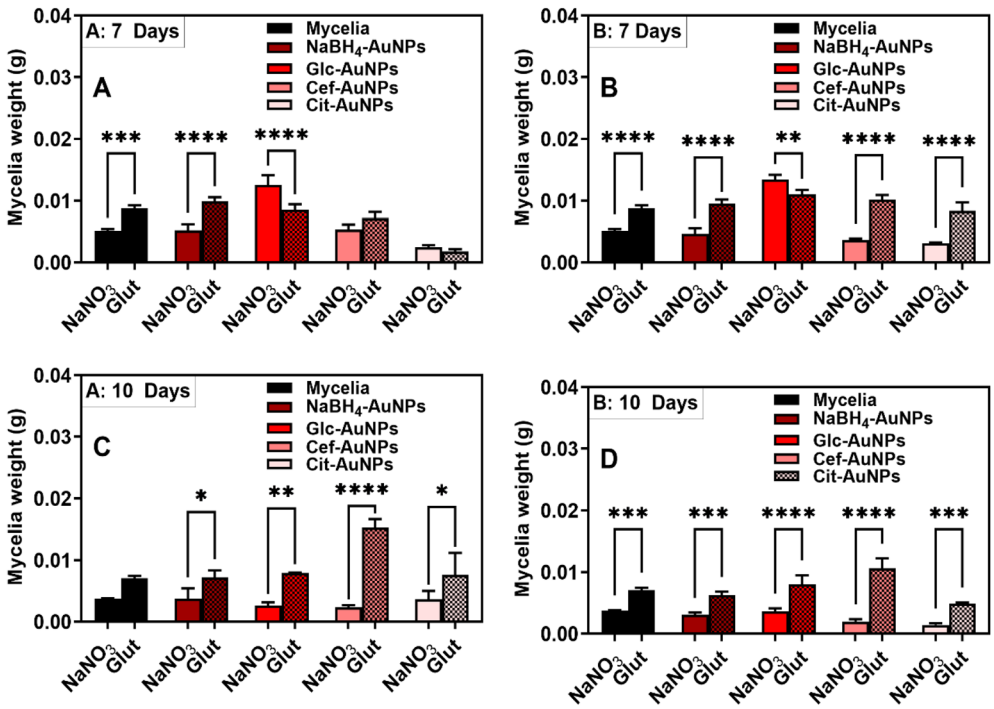

Fig. 3 Mycelia yield of *Aspergillus niger* with varying AuNP concentrations (20 or 30 μg mL^{-1}) over 7 or 10 days. (A) Glutamine: 20 or 30 μg mL^{-1} of AuNPs for 7 days; (B) glutamine: 20 or 30 μg mL^{-1} of AuNPs for 10 days; (C) nitrate: 20 or 30 μg mL^{-1} of AuNPs for 7 days; (D) nitrate: 20 or 30 μg mL^{-1} of AuNPs for 10 days. The level of significance: *($p \leq 0.05$), **($p \leq 0.01$), and ***($P \leq 0.001$).

offering extra nutrients to the fungus. This current observation is consistent with our previous report on stress characterization *via* melanin and biofilm assessment under the same NP groups.[15] Sporulation was reduced with glutamine as the nitrogen source (Fig. 2B), in agreement with previous studies indicating glutamine as a preferred nitrogen source for *A. niger's* growth.[30]

4.4 Optimization of conditions for the functionalization of *A. niger* with AuNPs

4.4.1 Impact of nitrogen source and AuNP concentration on mycelial yield. To evaluate how varying conditions affected the ability of *Aspergillus niger* to grow and form a well-defined mycelium for maximum interaction with the AuNPs, the mycelial yield was assessed under different concentrations of gold nanoparticles (AuNPs; 20 or 30 μg mL^{-1}) and nitrogen sources (nitrate or glutamine) over incubation periods of 7 or 10 days (Fig. 3). Significant variations in yield were observed depending on AuNP concentration, nitrogen source, and growth duration. Generally, higher AuNP concentrations led to lower yields, except for Glc-AuNPs, where yield was unaffected, probably due to additional nutrients from the glucose associated with the AuNPs. With glutamine as the nitrogen source, higher yields were produced at 30 μg mL^{-1} after 7 days (Fig. 3A), but no significant difference was noted after a longer growth time, except for Cef-AuNPs, which grew better at lower AuNP concentrations at longer incubation period (10 days) (Fig. 3B). For nitrate as a nitrogen source, the mycelial yield was mostly unaffected by growth duration or AuNP concentration (Fig. 3C and D). However, lower concentrations of Cit-AuNPs resulted in higher yields, suggesting an antifungal effect due to prolonged interaction (Fig. 3D).[31]

Overall, glutamine, as a nitrogen source, resulted in significantly higher yields compared to nitrate (Fig. SF5A–D), indicating that the nitrogen source had a greater impact on yield than AuNP concentration. Likewise, a greater quantity of nano materials was produced in the presence of Glc-AuNPs, suggesting that surface functionalization has a more significant impact than growth period.[30] A representative image of the *A. niger*–AuNP composites is presented in Fig. 4. SEM/EDX analyses confirmed successful AuNP functionalization of *A. niger* mycelia (Fig. SF6 and SF7). Uniform AuNP coatings were observed across all groups ($NaBH_4$-AuNPs, Glc-AuNPs, Cef-AuNPs, Cit-AuNPs) at 20 and 30 μg mL^{-1} concentrations, with slight particle clustering in Glc-AuNPs. EDX detected strong Au bands at 2.2 keV. Cit-AuNPs showed intense sporulation without damaging fungal spores. SEM/EDX results suggest natural coupling processes effectively form AuNP–*A. niger* composites without external agents.

4.4.2 Impact of nitrogen source and AuNP concentration on the extent of AuNP deposition on mycelia. To optimize AuNP deposition in the biofiltration matrix of nanoparticles and mycelia, we evaluated the effects of different nitrogen sources, AuNP concentrations, and growth durations on AuNP deposition. The goal was to enhance the surface area of AuNPs for improved mercury adsorption. We tested the ELM formation at 20 or 30 μg mL^{-1} of AuNPs over 7 or 10 days. ICPMS results

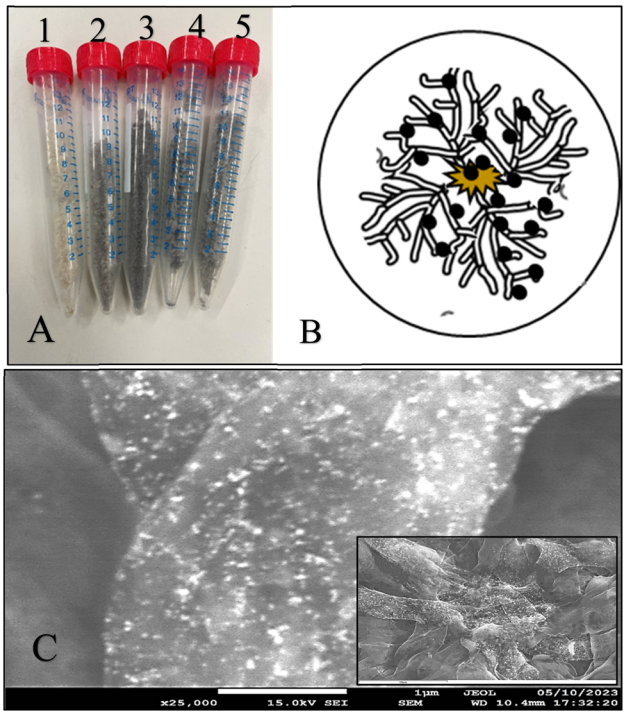

Fig. 4 Representative images of *A. niger*–AuNP composites. (A) Visual comparison of different *A. niger*–AuNP composites grown using glutamine as the nitrogen source. (1) control (no AuNPs), (2) mycelia with $NaBH_4$-reduced AuNPs, (3) mycelia with glucose-mediated AuNPs (Mycelia-Glc-AuNPs), (4) mycelia with cefaclor-mediated AuNPs (Mycelia-Cef-AuNPs), and (5) mycelia with citrate-mediated AuNPs (Mycelia-Cit-AuNPs). (B) Schematic illustration depicting the attachment of AuNPs to the fungal mycelia. (C). High magnification SEM image (scale bar represents 1 μM) showing the distribution of AuNPs on *A. niger* filament. The insert in Fig. 4C (scale bar represents 10 μM) shows a low-magnification SEM image depicting AuNPs deposition on multiple *A. niger* filaments.

(Fig. 5A–D) showed that a concentration of 30 μg mL^{-1} led to higher AuNP deposition, with greater accumulation over 10 days, regardless of the nitrogen source (glutamine or nitrate) (Fig. 5B and D).

To assess the impact of nitrogen sources (glutamine *vs.* nitrate) on AuNP deposition, we evaluated their effects under the same growth conditions (concentration and duration) (Fig. SF8A–D). Nitrate favoured deposition after 7 days (Fig. SF8A and B), while glutamine was preferred for Glc-AuNPs and $NaBH_4$-AuNPs after 10 days, and nitrate was favoured for Cef-AuNPs and Cit-AuNPs (Fig. SF7C and D). Strong interactions between the fungal mycelia and AuNPs, linked to their stability (Rasmussen *et al.*, 2020),[32] these were reflected in the zeta potential values: Cef-AuNPs: +41.5 ± 12.0, Cit-AuNPs: −41.3 ± 8.49, Glc-AuNPs: −38.5 ± 6.13, and $NaBH_4$-AuNPs: −35.7 ± 8.39 (Sadaf *et al.*, 2024).[15] This was consistent with SEM results, showing more uniform and unagglomerated microstructures (Fig. SF6).

Based on these results, we determined that the composite forms most effectively at 30 μg mL^{-1} AuNPs, with both nitrogen sources retained for further studies.

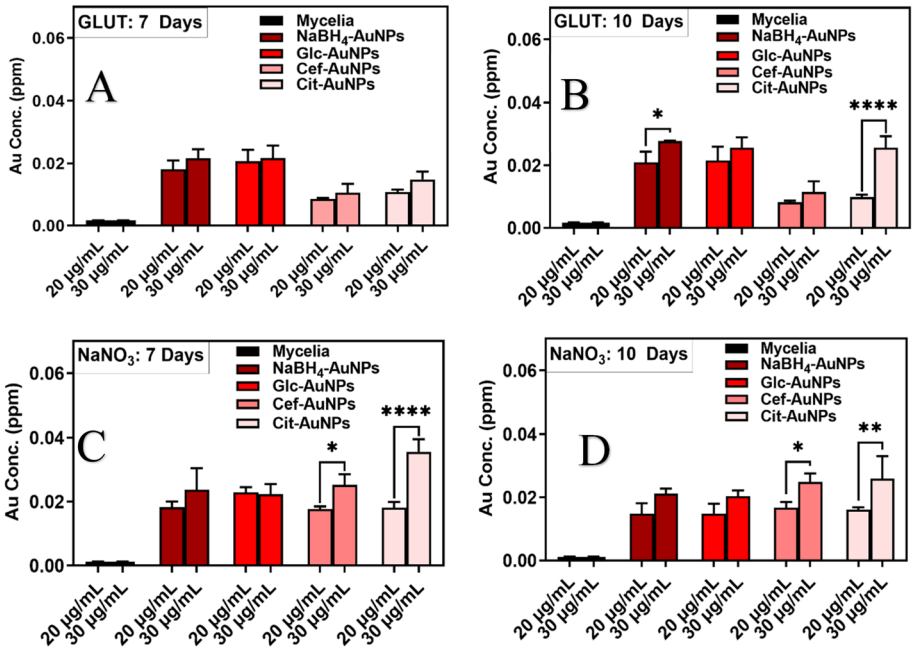

Fig. 5 AuNPs deposition on *A. niger* with varying AuNPs concentration (20 or 30 μg mL^{-1}) over 7 or 10 days. (A) Glutamine: 20 or 30 μg mL^{-1} of AuNPs for 7 days; (B) glutamine: 20 or 30 μg mL^{-1} of AuNPs for 10 days; (C) nitrate: 20 or 30 μg mL^{-1} of AuNPs for 7 days; (D) nitrate: 20 or 30 μg mL^{-1} of AuNPs for 10 days. The level of significance: *($p \leq 0.05$), **($p \leq 0.01$), and ***($P \leq 0.001$).

4.5 Filtration efficiency of AuNPs-functionalized mycelial composites for mercury removal

After optimising the conditions, we explored the ability of fungal mycelial composites formation created at 30 μg mL^{-1} of AuNPs, grown for 10 days using nitrate or glutamine as nitrogen sources, as reusable filters for mercury removal. From our mercury filtration experiments, mercury binds strongly to gold, possibly through amalgamation.[33] These biofilters were compared to a commercial industrial filter (Pierce™ Centrifuge Column with a polyethylene filter and a 30 μm pore size) and a control sample, mycelial material grown under identical conditions, except for the presence of the AuNPs. Cef-AuNP and Cit-AuNP-mycelial composites were effective under both nitrogen conditions (Fig. 6A and B), though materials grown in the presence of glutamine as the nitrogen source were most effective (Fig. 6A). Glc-AuNPs and $NaBH_4$-AuNPs showed improved performance with glutamine as the nitrogen source, with the filtration efficiency of the $NaBH_4$-AuNPs-mycelia composite being much reduced and very similar to the control with no gold NPs present. It is noteworthy that the mycelia alone were able to achieve a certain degree of filtration. The Glc-AuNPs, Cef-AuNPs, and Cit-AuNPs mycelial composites effectively reduced mercury levels, achieving removal rates of up to 90% from an initial concentration of 5 ppb in certain groups. Despite its sensitivity to mercury detection on its own, $NaBH_4$-AuNPs showed no significant filtration effects when combined with mycelia. Glc-AuNPs were only effective with glutamine as the nitrogen source. Consequently, $NaBH_4$-AuNPs and Glc-AuNPs mycelia composites grown in the presence of nitrate as the nitrogen source, and $NaBH_4$-AuNPs-mycelia composites grown in the presence of glutamine as the nitrogen source, were excluded from further studies. The remaining groups were tested over five filtration periods to evaluate their reusability.

According to WHO,[8] mercury removal from water down to 1 ppb can be achieved using methods like coagulation/sedimentation/filtration, Poly Aluminium Chloride (PAC), and ion exchange. Previous methods in the UK achieved up to 52.2% removal during primary treatment and 29.5% during secondary treatment.[34] Our system offers significant improvements, especially for low-level contaminated waters, fitting regulatory requirements in countries with stringent maximum acceptable concentration (MAC) for mercury.[35,36]

4.6 Reusability of the composite in mercury filtration

Initial experiments showed the effectiveness of certain AuNPs-fungal composite filters in mercury filtration, leading to their selection for reusability screening. Results from five runs (Fig. 7A and B) showed mercury concentration dropped below 2 ppb, the United States Environmental Protection Agency's maximum allowed concentration (USEPA MAC) for mercury in wastewater.[37] Composites grown in the presence of glutamine (Glc-AuNPs, Cef-AuNPs, Cit-AuNPs) effectively remove mercury over five reuse cycles, demonstrating efficiency and reusability (Fig. 7A). Composites grown in the presence of nitrate (Cit-AuNPs, Cef-AuNPs) showed varying responses, with Cef-AuNPs becoming more efficient over time (Fig. 7B). Materials grown in the presence of both nitrogen sources reduced mercury to the WHO MAC over repeated use. Mycelia composites can serve as novel filtration systems for reducing mercury concentrations in wastewater to levels below the WHO MAC. Differing behaviour under the different nitrogen sources suggests that factors like

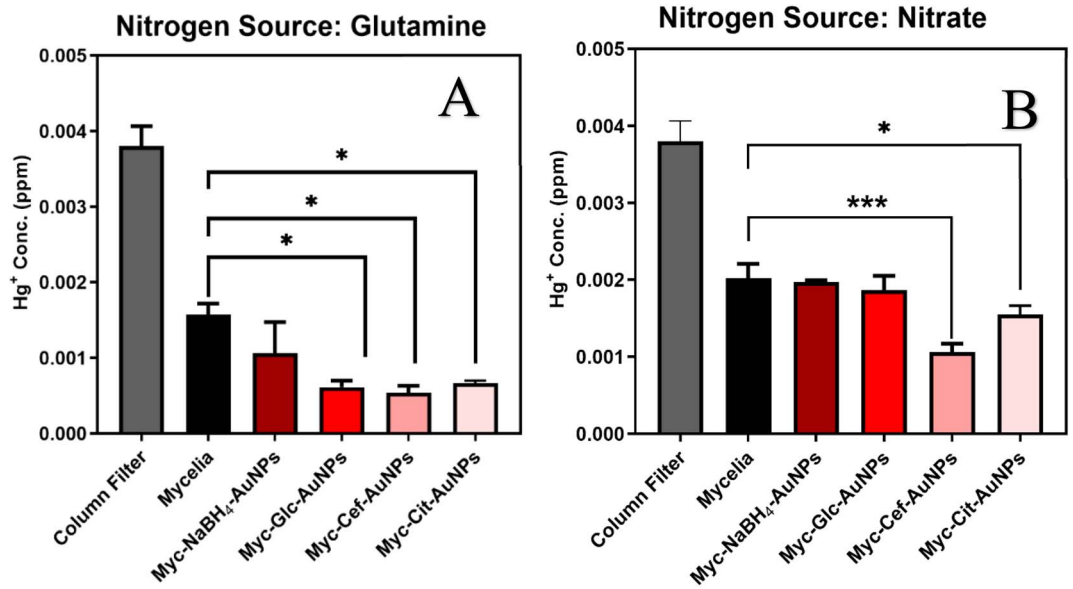

Fig. 6 Quantitative comparison of Hg^{2+} removed by *Aspergillus niger* mycelia after 30 minutes of interaction at 30 μg mL^{-1} when either glutamine (A) or nitrate (B) was used as a nitrogen source in the growth of the mycelia. The level of significance: *($p \leq 0.05$), **($p \leq 0.01$), and ***($P \leq 0.001$). The starting level of mercury is 5 ppb.

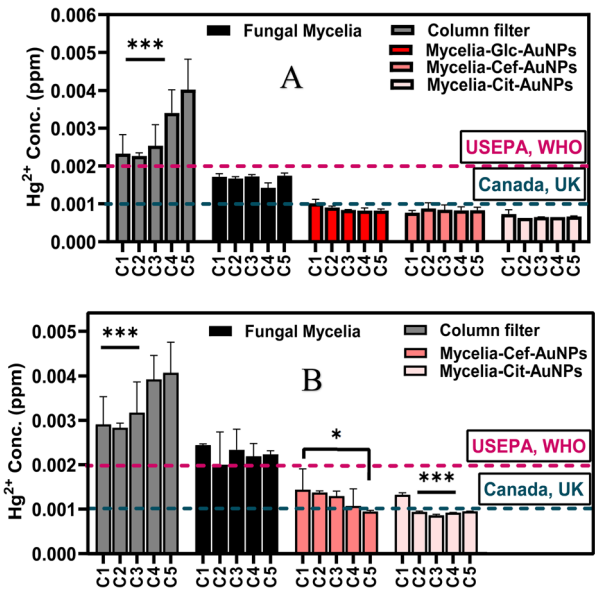

Fig. 7 Mercury filtration (from a 5-ppb solution) using AuNPs-mycelia composites over five washes when the nitrogen source was (A) glutamine and (B) nitrate.

surface-free energy and wettability influence filtration effectiveness. For example, our surface chemistry analysis (SF3) suggests stronger interactions when glutamine is used as the nitrogen source. This aligns with our experimental outcomes: the glutamine-grown group was more effective in mercury filtration. This finding indicates that both effectiveness and reusability of the composite can be tuned at a fundamental level through nutrient modification, offering promising potential for future translational applications.

4.7 Recycling mercury from AuNPs-mycelia composite

After confirming the reusability over five cycles without structural deformation of the mycelial-based material, we explored mercury recycling from the composites using ddH_2O pH 8.0 desorption (Jing, *et al.*, 2007). Our results, presented in Fig. 8A

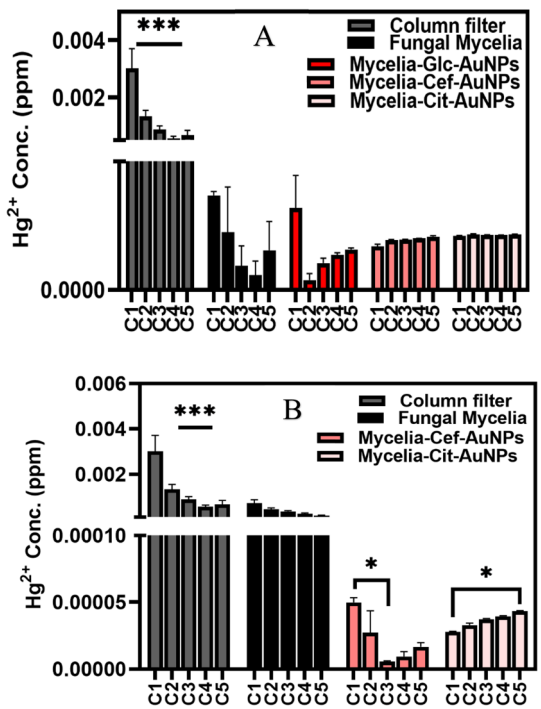

Fig. 8 Mercury desorption from AuNPs-mycelia composites over five washes when the nitrogen source was (A) glutamine and (B) nitrate. The starting level of mercury is 5 ppb.

Table 2 Mercury recovery rates from AuNPs-mycelial composites over five desorption cycles

Sample	Hg^{2+} recovery (%)
Glutamine	
Column filter	63.80
A. niger mycelia	0.32
Glc-AuNPs-mycelia	0.22
Cef-AuNPs-mycelia	0.28
Cit-AuNPs-mycelia	0.30
Nitrate	
Column filter	66.84
A. niger mycelia	14.06
Cef-AuNPs-mycelia	0.53
Cit-AuNPs-mycelia	0.90

and B, showed progressive mercury desorption over five washes depending on nitrogen sources (glutamine or nitrate). The percentages removed are presented in Table 2. We initially hypothesized that ddH_2O pH 8.0 desorption would be effective based on the work of Jing *et al.*,[38] who demonstrated that similar conditions facilitated the desorption of heavy metals using pH adjustments. However, our results indicate that the interaction between the mycelial-based composites and mercury is stronger than anticipated, leading to lower recovery rates, creating the need for an alternative desorption system or more desorption cycles. This underscores the eco-friendly potential of fungi in addressing heavy metal pollution and the importance of applied mycology intersecting with nanotechnology.

4.8 Study significance, limitations, and future directions

Generally, unlike conventional filters that often require controlled environments or chemical pre-treatment, our biofilter operates through direct interaction with contaminants, without external energy input or complex infrastructure. Its non-rigid, adaptable structure allows deployment in diverse settings. Additionally, the material is reusable with progressive recyclability, offering long-term cost and environmental benefits. This research bridges gaps in mercury remediation and advances sustainable practices through the innovative integration of fungal materials and nanotechnology. However, this study serves as a proof of concept specifically for mercury ions; future work should explore performance in complex media and with other contaminants to assess broader selectivity and applicability.

5 Conclusion

This study focused exclusively on *A. niger* for mercury bioremediation, and findings may not apply to other strains or pollutants. The effects of varying nitrogen sources (nitrate and glutamine) on biofilter yield and efficiency were documented. This study demonstrated the potential of *A. niger* mycelia functionalized with gold nanoparticles (AuNPs) as sustainable, reusable biofilters for mercury bioremediation. The composite material effectively detected and removed mercury to levels below the WHO maximum allowable limit. Key findings include the significant influence of nanoparticle concentration, nitrogen source, and growth duration on AuNP deposition, with glutamine enhancing mycelial yield and AuNP deposition, while nitrate favoured specific AuNP functionalization. AuNP exposure increased sporulation, particularly with nitrate, aiding nanoparticle integration. The biofilters outperformed conventional industrial filters in mercury removal efficiency, and their reusability and mercury recovery potential highlight their eco-friendly and cost-effective attributes.

Author contributions

Carole Perry was responsible for conceptualizing the research idea, designing the experimental approach, supervising the project, guiding data interpretation, and critically revising the manuscript. Juwon Samuel Afolayan carried out all experimental work and data collection, developed and optimized methodologies, performed formal data analysis and visualization, and drafted the manuscript. Both authors confirmed the final version of the manuscript.

Conflicts of interest

The authors declare that there are no conflicts of interest affecting the research, analysis, or conclusions presented in this paper.

Data availability

All data supporting this study has been included in the paper and/or the SI. See DOI: **https://doi.org/10.1039/d5su00556f**.

Acknowledgements

CCP acknowledges funding provided by AFOSR FA9550-20-1-0206 and FA9550-24-1-0274. JSA is thankful for the financial support of his studies through a vice-chancellor's scholarship from Nottingham Trent University. The authors also appreciate the assistance from the central facility at Nottingham Trent University with ICP-MS, X-ray analysis, and the support from the Medical Technologies Innovation Facility (MTIF) at the Clifton campus for SEM-EDAX studies.

References

1 S. N. Zulkifli, H. A. Rahim and W. J. Lau, Detection of contaminants in water supply: A review on state-of-the-art monitoring technologies and their applications, *Sens. Actuators, B*, 2018, **255**, 2657–2689, DOI: **10.1016/j.snb.2017.09.078**.

2 F. Cutrupi, A. D. Osinska, I. Rahmatika, J. S. Afolayan, Y. Vystavna, O. Mahjoub, J. I. Cifuentes, D. Pezzutto and W. Muziasari, Towards monitoring the invisible threat: a global approach for tackling AMR in water resources and

environment, *Front. Water*, 2024, **6**, 1362701, DOI: 10.3389/frwa.2024.1362701.

3 E. O. Ajani, J. S. Afolayan and S. Sabiu, Characterization of Blighia sapida synthesized-copper nanoparticle and its application in periodic pharmaceutical effluent treatment, *J. Environ. Sci. Health, Part A*, 2021, **56**(5), 508–515, DOI: 10.1080/10934529.2021.1890497.

4 V. K. Parida, D. Sikarwar, A. Majumder and A. K. Gupta, An assessment of hospital wastewater and biomedical waste generation, existing legislations, risk assessment, treatment processes, and scenario during COVID-19, *J. Environ. Manage.*, 2022, **308**, 114609, DOI: 10.1016/j.jenvman.2022.114609.

5 M. Zaynab, R. Al-Yahyai, A. Ameen, Y. Sharif, L. Ali, M. Fatima, K. A. Khan and S. Li, Health and environmental effects of heavy metals, *J. King Saud Univ. Sci.*, 2022, **34**(1), 101653, DOI: 10.1016/j.jksus.2021.101653.

6 M. Ahmed, M. O. Mavukkandy, A. Giwa, M. Elektorowicz, E. Katsou, O. Khelifi, V. Naddeo and S. W. Hasan, Recent developments in hazardous pollutants removal from wastewater and water reuse within a circular economy, *npj Clean Water*, 2022, **5**(1), 1–25, DOI: 10.1038/s41545-022-00154-5.

7 J. Georgin, D. S. Franco, Y. Dehmani, P. Nguyen-Tri and N. El Messaoudi, Current status of advancement in remediation technologies for the toxic metal mercury in the environment: A critical review, *Sci. Total Environ.*, 2024, **5**, 174501, DOI: 10.1016/j.scitotenv.2024.174501.

8 World Health Organization, Guidelines for drinking-water quality, *WHO Chron.*, 2011, **38**(4), 104–108.

9 L. Wang, W. Ma, L. Xu, W. Chen, Y. Zhu, C. Xu and N. A. Kotov, Nanoparticle-based environmental sensors, *Mater. Sci. Eng., R*, 2010, **70**(3–6), 265–274, DOI: 10.1016/j.mser.2010.06.012.

10 A. R. de Araujo Scharnberg and F. Ravanello, Wastewater Treatment Using Nanomaterials, *Environ. Appl. Nanomater.*, 2022, 17–31, DOI: 10.1007/978-3-030-86822-2_2.

11 I. G. Wawata, and O. A. Fabiyi, Sustainable application of nanomaterials in the removal of heavy metals from water, in *Sustainable Nanomaterials: Synthesis and Environmental Applications*, Springer Nature Singapore, Singapore, 2024, 21, pp. 21–44, DOI: 10.1007/978-981-97-2761-2_2.

12 D. Kirubakaran, J. B. Wahid, N. Karmegam, R. Jeevika, L. Sellapillai, M. Rajkumar and K. J. SenthilKumar, A comprehensive review on the green synthesis of nanoparticles: advancements in biomedical and environmental applications, *Biomed. Mater. & Devices*, 2025, **24**, 1–26, DOI: 10.1007/s44174-025-00295-4.

13 T. Bohu, R. Anand, R. Noble, M. Lintern, A. H. Kaksonen, Y. Mei, K. Y. Cheng, X. Deng, J. P. Veder, M. Bunce and M. Power, Evidence for fungi and gold redox interaction under Earth surface conditions, *Nat. Commun.*, 2019, **10**(1), 2290, DOI: 10.1038/s41467-019-10006-5.

14 R. Yu, M. Li, Y. Wang, X. Bai, J. Chen, X. Li, H. Wang and H. Zhang, Chemical investigation of a co-culture of *Aspergillus* fumigatus D and Fusarium oxysporum R1, *Rec. Nat. Prod.*, 2021, **15**, 130–135, DOI: 10.25135/rnp.199.20.07.172.

15 A. Sadaf, J. S. Afolayan and C. C. Perry, Developing gold nanoparticle mycelial composites: Effect of nanoparticle surface functionality on *Aspergillus niger* viability and cell wall biochemistry, *Curr. Res. Biotechnol.*, 2024, **7**, 100185, DOI: 10.1016/j.crbiot.2024.100185.

16 S. Krappmann and G. H. Braus, Nitrogen metabolism of *Aspergillus* and its role in pathogenicity, *Med. Mycol.*, 2005, **43**(Supplement_1), S31–S40, DOI: 10.1080/13693780400024271.

17 K. Hayer, M. Stratford and D. B. Archer, Germination of *Aspergillus niger* conidia is triggered by nitrogen compounds related to L-amino acids, *Appl. Environ. Microbiol.*, 2014, **80**(19), 6046–6053, DOI: 10.1128/AEM.01078-14.

18 X. Shao, D. Yang, M. Wang and Q. Yue, A colorimetric detection of Hg2+ based on gold nanoparticles synthesized oxidized N-methylpyrrolidone as a reducing agent, *Sci. Rep.*, 2023, **13**(1), 22208, DOI: 10.1038/s41598-023-49551-x.

19 J. W. Park and J. S. Shumaker-Parry, Structural study of citrate layers on gold nanoparticles: role of intermolecular interactions in stabilizing nanoparticles, *J. Am. Chem. Soc.*, 2014, **136**(5), 1907–1921, DOI: 10.1021/ja4097384.

20 R. Farajollah, M. M. Nikje, E. Saadat and F. A. Dorkoosh, Star-hyperbranched waterborne polyurethane based on D-glucose-poly (ε-caprolactone) core as a biomaterial candidate, *Eur. Polym. J.*, 2021, **147**, 110318, DOI: 10.1016/j.eurpolymj.2021.110318.

21 S. Suvarna, U. Das, S. Kc, S. Mishra, M. Sudarshan, K. D. Saha, S. Dey, A. Chakraborty and Y. Narayana, Synthesis of a novel glucose capped gold nanoparticle as a better theranostic candidate, *PLoS One*, 2017, **12**(6), e0178202, DOI: 10.1371/journal.pone.0178202.

22 G. W. Wu, S. B. He, H. P. Peng, H. H. Deng, A. L. Liu, X. H. Lin, X. H. Xia and W. Chen, Citrate-capped platinum nanoparticle as a smart probe for ultrasensitive mercury sensing, *Anal. Chem.*, 2014, **86**(21), 10955–10960, DOI: 10.1021/ac503544w.

23 T. Lou, L. Chen, C. Zhang, Q. Kang, H. You, D. Shen and L. Chen, A simple and sensitive colorimetric method for detection of mercury ions based on anti-aggregation of gold nanoparticles, *Anal. Methods*, 2012, **4**(2), 488–491, DOI: 10.1039/C2AY05764F.

24 B. P. Nanda, P. Rani, P. Paul, S. S. Ganti and R. Bhatia, Recent trends and impact of localized surface plasmon resonance (LSPR) and surface-enhanced Raman spectroscopy (SERS) in modern analysis, *J. Pharm. Anal.*, 2024, **14**(11), 100959, DOI: 10.1016/j.jpha.2024.02.013.

25 A. J. Mwakalesi and M. J. Nyangi, Colorimetric Sensing of Mercury in Aqueous Solutions Using Silver Nanoparticles Prepared from Synadenium glaucescens Root Aqueous Extract, *Eng. Proc.*, 2023, **56**(1), 182, DOI: 10.3390/ASEC2023-15310.

26 P. C. Yang, T. Wu and Y. W. Lin, Label-free colorimetric detection of mercury (II) ions based on gold nanocatalysis, *Sensors*, 2018, **18**(9), 2807, DOI: 10.3390/s18092807.

27 B. P. Nanda, P. Rani, P. Paul, S. S. Ganti and R. Bhatia, Recent trends and impact of localized surface plasmon resonance (LSPR) and surface-enhanced Raman spectroscopy (SERS) in modern analysis, *J. Pharm. Anal.*, 2024, **14**(11), 100959, DOI: **10.1016/j.jpha.2024.02.013**.

28 J. A. Nychka and M. M. Gentleman, Implications of wettability in biological materials science, *Jom*, 2010, **62**, 39–48, DOI: **10.1007/s11837-010-0107-6**.

29 B. Tudzynski, Nitrogen regulation of fungal secondary metabolism in fungi, *Front. Microbiol.*, 2014, **5**, 656, DOI: **10.3389/fmicb.2014.00656**.

30 M. Novodvorska, K. Hayer, S. T. Pullan, R. Wilson, M. J. Blythe, H. Stam, M. Stratford and D. B. Archer, Transcriptional landscape of *Aspergillus niger* at breaking of conidial dormancy revealed by RNA-sequencing, *BMC Genomics*, 2013, **14**, 1–8, DOI: **10.1186/1471-2164-14-246**.

31 K. A. Eid, H. F. Salem, A. A. Zikry, A. F. El-Sayed and M. A. Sharaf, Antifungal effects of colloidally stabilized gold nanoparticles: screening by microplate assay, *Nat. Sci.*, 2011, **29**(2), 29–33.

32 M. K. Rasmussen, J. N. Pedersen and R. Marie, Size and surface charge characterization of nanoparticles with a salt gradient, *Nat. Commun.*, 2020, **11**(1), 2337, DOI: **10.1038/s41467-020-15889-3**.

33 A. K. Donkor, H. Ghoveisi and J. C. Bonzongo, Use of metallic mercury in artisanal gold mining by amalgamation: a review of temporal and spatial trends and environmental pollution, *Minerals*, 2024, **14**(6), 555, DOI: **10.3390/min14060555**.

34 A. J. Hargreaves, P. Vale, J. Whelan, C. Constantino, G. Dotro and E. Cartmell, Mercury and antimony in wastewater: fate and treatment, *Water, Air, Soil Pollut.*, 2016, **227**, 1–17, DOI: **10.1007/s11270-016-2756-8**.

35 The United Kingdom Government, *The Water Supply (Water Quality) Regulations 2016*, The United Kingdom Government, 2016, **https://www.legislation.gov.uk/uksi/2016/614/contents**.

36 Health Canada, *Guidelines for Canadian Drinking Water Quality: Guideline Technical Document – Mercury*, Health Canada, 1979, **https://www.canada.ca/en/health-canada/services/publications/healthy-living/guidelines-canadian-drinking-water-quality-guideline-technical-document-mercury.html**.

37 World Health Organization, *Mercury in Drinking-Water Background Document for Development of WHO Guidelines for Drinking-Water Quality*, 2017, **https://www.who.int/docs/default-source/wash-documents/wash-chemicals/mercury-background-document.pdf?sfvrsn=9b117325_4**.

38 Y. D. Jing, Z. L. He and X. E. Yang, Effects of pH, organic acids, and competitive cations on mercury desorption in soils, *Chemosphere*, 2007, **69**(10), 1662–1669, DOI: **10.1016/j.chemosphere.2007.05.033**.